NASA TECHNICAL MEMORANDUM NASA TM-77080

A TUNABLE DUAL FREQUENCY DYE LASER DUAL FREQUENCY OSCILLATOR DESIGN

Y. Aubry

Translation of "Laser à colorant bifrequence accordable," Office National d'Etudes et de Recherches Aérospatiales, Toulouse (France). Dept. d'Etudes et de Recherches en Optique; (ONERA-DERO-1/6083-3), Dec. 11, 1981, 43 pp.

NATIONAL AERONAUTICS AND SPACE ADMINISTRATION
WASHINGTON, D.C. 20546 MAY 1983

STANDARD TITLE PAGE

1. Report No.	2. Government Accession No.	3. Recipient's Catalog No.
NASA TM-77080		

4. Title and Subtitle	5. Report Date
A TUNABLE DUAL FREQUENCY DYE LASER - DUAL FREQUENCY OSCILLATOR DESIGN.	May 1983
	6. Performing Organization Code

7. Author(s)	8. Performing Organization Report No.
Y. Abury	
	10. Work Unit No.

9. Performing Organization Name and Address	11. Contract or Grant No.
Leo Kanner Associates Redwood City, CA 94063	NASW-3541
	13. Type of Report and Period Covered
12. Sponsoring Agency Name and Address	Translation
National Aeronautics and Space Administration, Washington, D.C. 20546	14. Sponsoring Agency Code

15. Supplementary Notes

Translation of "Laser à colorant bifréquence accordable," Office National d'Etudes et de Recherches Aérospatiales, Toulouse (France), Dept. d'Etudes et de Recherches en Optique, (ONERA-DERO-1/6083-3), Dec. 11, 1981, 43 pp. (N82-32725).

16. Abstract The pulsed dye laser offers a tunable oscillator, followed by three amplifiers. It is pumped by a dual frequency Nd-Yag laser. Tuning and spectral width are controlled by a holographic network connected to a high power telescope. The modified two-wavelength dye laser allows for absorption lidar techniques for remote sensing of the atmosphere. Line switching is achieved by electro-optical commutation. The study began by first performing a feasiblity experiment with the original oscillator. A model was then built, and tested with different dyes. After a few modifications were made to improve the conversion efficiency, this oscillator was inserted in the laser to check whether the amplifier stages were correctly adjusted.

17. Key Words (Selected by Author(s))	18. Distribution Statement
tunable laser, dye laser, pulsed laser, laser metrology, Lidar, atmospheric sensing	Unclassified-Unlimited

19. Security Classif. (of this report)	20. Security Classif. (of this page)	21. No. of Pages	22.
Unclassified	Unclassified		

ABSTRACT

The adjustment of an oscillator capable of emitting two virtually simultaneous tunable spectral lines, broadens the capabilities of lidar techniques for remote sensing of the atmosphere with a view to differential absorption experiments.

The dual frequency oscillator of this study does not have any mobile mechanical part. Its performances are described along with the performance achieved after a power dye laser is inserted.

TABLE OF CONTENTS

A TUNABLE DUAL FREQUENCY DYE LASER - DUAL FREQUENCY OSCILLATOR DESIGN

Y. Aubry
Optical Research and Studies Division

INTRODUCTION /1

The pulsed dye laser, built by the Jobin-Yvon company under C.N.E.S. contract, is made up of a tunable oscillator, followed by three amplifiers. It is pumped by a dual frequency Nd-YAG laser.

Tuning along with spectral width are controlled by a holographic network, or grating, connected to a high power telescope.

The laser was modified to include the capability of sending two wavelengths to permit its use for differential absorption techniques. Line switching is achieved by electro-optical commutation.

The study began by performing a feasiblity experiment with the original oscillator. A model was then built, and tested with different dyes. Following a few modifications made to improve the conversion efficiency, this oscillator was inserted in the laser to check for a fine adjustment of the amplifier stages.

I - OSCILLATOR /3

I - 1. General Design Of The Dual Frequency Oscillator (figure 1).

The basic components of the cavity of a tunable oscillator are:

-the dye tank,

*Numbers in the margin indicate pagination in the original text.

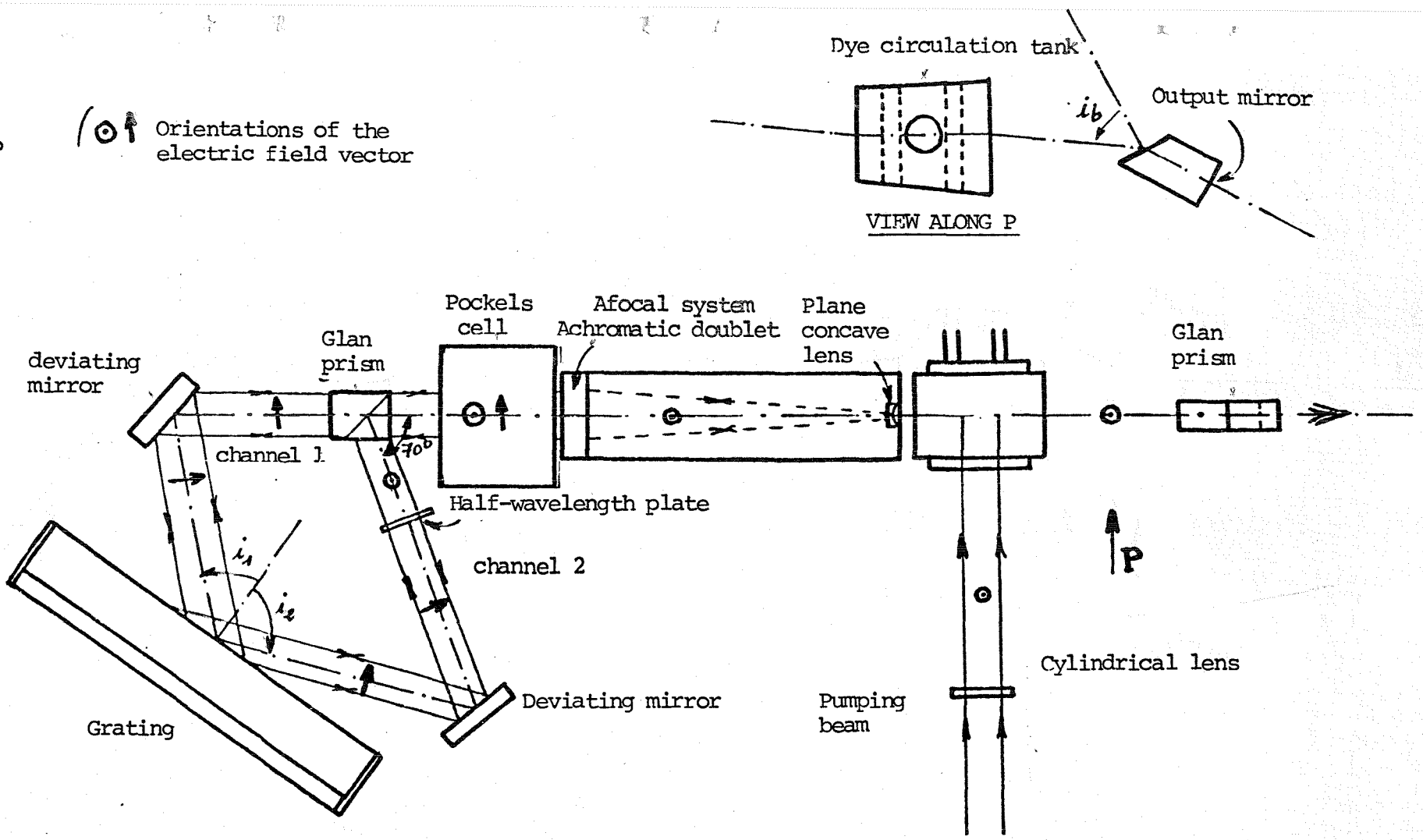

Figure 1 - Diagram Of The Dual Frequency Oscillator
(scale: 0.5)

-the network (grating),
-the output mirror.

The dual frequency oscillator is made by using a single Littrow grating and a Glan prism. The incidence on the grating falls to the right or to the left of the axis, depending on whether the polarization state of the light from the tank is s or p. In both cases, the angles of incidence, and therefore the wavelengths, are fixed by the position of the deviating mirror. If the beam is deflected by the Glan prism (polarization s), a half-wave plate restores the electrical field vector perpendicular to the grating lines to bring the latter to its maximum efficiency.

To obtain the required conversion efficiency, the electrical fields of the pumping beam and of the oscillator beam must be colinear in the tank. Considering the system configuration, this direction is parallel to the grating lines. To make it convenient to initiate the oscillation along this direction, a polarizer is placed in the cavity. One of its faces is cut to the Brewster's angle so as it minimize losses. The other faces serves as an output mirror.

The spectral line emitted is finer when more numerous grating lines are illuminated on the grating. The role of the afocal system is to widen the beam for this purpose.

As the electrical field has a fixed direction from the dye tank side, the wave length is modified using a Pockel's cell operating in a half-wave. This means that when it is fed with the required voltage, it makes the electrical field rotate by 90 degrees. This cell is placed between the afocal and the Gland prism, because /4

the energy density in it is much lower there than between the afocal and the dye tank.

Finally, the pumping beam, after the sampling plate, is focused on the dye with a cylindrical lens. Afterward, when the light beam in the oscillator will not be deflected by the Glan prism, we will say that it oscillates over channel 1 to which the wavelength γ_1 will correspond. When the beam will be deflected, wavelength γ_2 will correspond to channel 2.

These are the spectral characteristics of the oscillator which will determine those of the laser. The emmision of a spectral line will remain very stable in the test conditions (airborne or spatial) and these conditions will be much harder to achieve with finer spectral lines.

Furthermore, the equipment's field of action depends on the spectral range in which the oscillator may emit, it is therefore important to achromatize it as far as possible.

These two points will be studied in the following paragraph.

I - 2. Oscillator Components

The magnification of the telescope being G, the tolerances for setting the rotating position of the components on either side of the telescope will be in the same ratio.

I - 2.1. Grating And Deviating Mirror

The divergence of a light beam having a γ wavelength,

depends on the luminous intensity distribution in a straight section of this beam. If the Glan prism limits the oscillator beam by a square side profile a and if the illumination there is uniform, the energy distribution with respect to the direction varies with the function $(\sin c)^2$. /5

$$F = \left| \frac{\sin \frac{\pi \alpha a}{\lambda}}{\frac{\pi \alpha a}{\lambda}} \right|^2$$

If we take into account only the rays for which $F > 0.5$, i.e. for which

$\frac{\pi \alpha}{\lambda}$ is less than or equal to 1.39,

the mid-height divergence of the beam is equal to

$$\delta = \frac{0.88\lambda}{a} \qquad (1)$$

In practice, a = 15 mm and for λ = 600 nm, we find δ = 7.2 arc seconds.

We call θ_M the angle of incidence on the mirror, θ_R, the angle of incidence on the grating and N the number of grating lines per millimeter of grating. The wavelength emitted by the oscillator is defined by:

$$\lambda = \frac{2\sin \theta_R}{N} \qquad (2)$$

The relationship between the wavelength variations and the angle of incidence variations on the grating are obtained by differentiating (2)

$$d\lambda = \frac{2\cos\theta}{N} d\theta_R \qquad (3)$$

As the grating is fixed, if one of the deviating mirrors pivots about a vertical or horizontal axis, of an angle $d\theta_M$, the angle of incidence on the grating varies by: /6

$$d\theta_R = 2\theta_M \qquad (4)$$

The fineness for a single passage of the spectral line emitted is obtained by calculating the ratio of relationships (2) and (3):

$$\frac{\lambda}{d\lambda} = \frac{a\ tg\theta_R}{0.88\lambda}$$

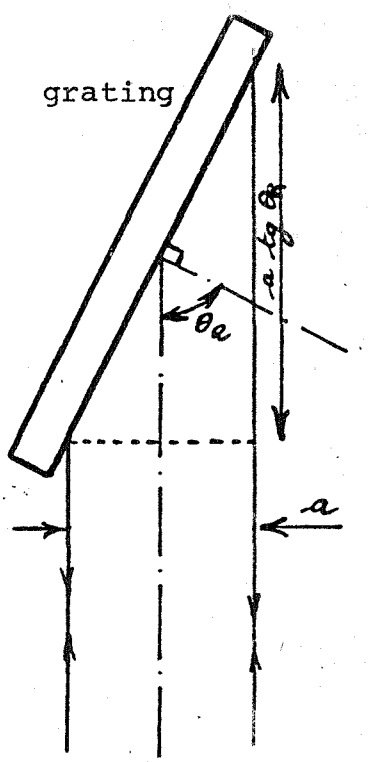

Figure 2
Path Difference

Figure 2 shows that the maximum path difference in the cavity, if the beam is recirculated several times and if the grating limitation is not included, is:

$$\ell = 2a\ tg\ \theta_R \qquad (7)$$

This lets us express relationship (6) in a form common to all dispersive systems:

$$(1.76)\ \lambda^2 = \ell\, d\lambda$$

The variations of the angle of incidence along both axes of the grating must be less than δ and, if we account for the number n of passages, the adjustment and stability of each

of the deviating mirrors should be assured with:

$$| d\theta_M | \text{ is less than or equal to } \frac{0.44\lambda}{\text{year}} \qquad (8)$$

Actually, the luminous intensity distribution at the Glan prism level is far from being uniform and the divergence is therefore greater. If we let L be the length of the oscillator cavity computed on the axis, Δt the pump pulse time and c the velocity of light, then the value of n is limited to the right:

$$n \text{ is less than or equal to } \frac{c\Delta t}{2L}$$

In practice, L = 0.55 m, Δt = 20 ns. We find that the number of round-trip passages in the cavity is less than or equal to 5 and that the adjustment and stability of the deviating mirrors should be assured at ±0.7 arc seconds.

There is another important point concerning the grating. The wavelength emitted is dependent upon N (number of grating lines per millimeter) according to relationship (2). If the temperature varies by Δt, the variations of ΔN for a linear expansion coefficient α of the grating support length L are given by:

$$\Delta N = - N\alpha \ \Delta t$$

and the relative wavelength variation is associated with the grating expansion by:

$$\frac{\Delta\lambda}{\lambda} = \alpha\Delta t$$

This means that if the ultimate performance of the

oscillator is an emission of 0.1 pm at 600 nm, the material upon which the grating is deposited must have an expansion coefficient so that:

$$\alpha \, \Delta t \text{ is less than or equal to } 1.7.10^{-7}$$

The two gratings were made on a material having a zero hardness factor.

I - The Pockel's Cell /8

When the cell is not on, the KDP crystal behaves like a uniaxial plate cut perpendicular to the optical axis (figure 3). A nonpolarized ray, incident with angle i, gives two emitted rays polarized at a right angle, whose path difference is:

$$\delta = e(KK'),$$

whose expression as a function of n_o and n_e is expressed:

$$\delta = \frac{1}{2} n_o i^2 \quad e\left(\frac{1}{n_o^2} - \frac{1}{n_e^2}\right.$$

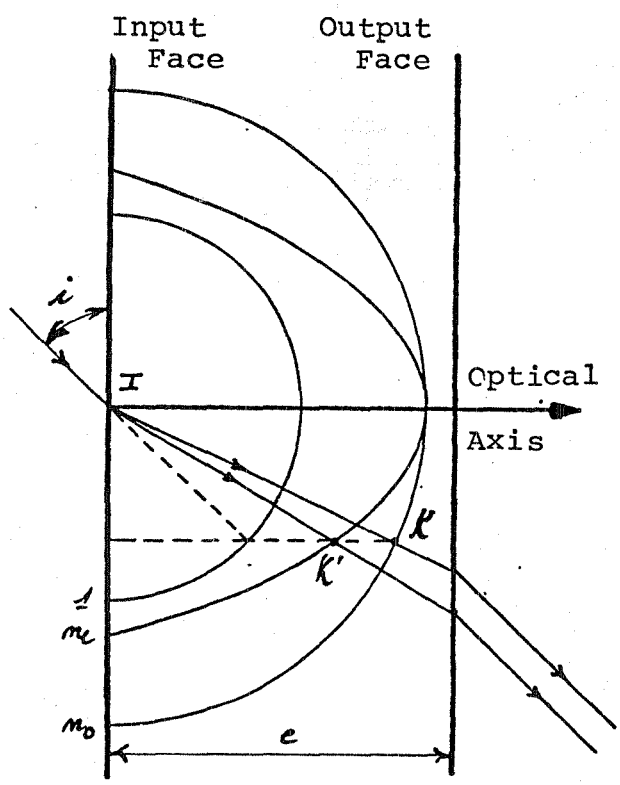

Figure 3 - Refraction in KD*P.

The fringes observed between the cross-polarizers are analogous to Newton's rings. The neutral lines are the directions parallel and perpendicular to the polarizer axes. The measurement of

of the angular dimension in the figure showing the interferences at the center of the field gives the tolerance of the Pockels cell orientation.

The irradiance in the observation plane of the fringes varies with:

$$\cos^2 \frac{\pi \delta}{\lambda}$$

If the extinction or transmission must be kept at a maximum value of about 0.01, δ must remain less than 0.03, and therefore i should not exceed ±5 degrees.

When the cell is live, the KDP crystal becomes bi-axial (figure 4). The longitudinal electro-optical effect is expressed by a variation of index Δ_n associated with the electrical field E by the relationship:

$$\Delta_n = - n^3 \, r \, E$$

If V is the voltage applied to the crystal and ℓ its length, E is given by:

$$E = \frac{V}{\ell}$$

In our particular case, n = 1.509, r = 25.10^{-12} m/V and ℓ = 23 mm. The index variation for a high voltage of 3.4 KV (value used in our experiments) is $\Delta n = 1.27.10^{-5}$. For a radius perpendicular to the input face, the optical path variation equals $\Delta\delta$ = 0.20 µm, a value which is very close to $\frac{\lambda}{2}$ for the wavelength of the sodium line which the oscillator is tuned to. It is not necessary for the path difference for the wavelength of channel 2 to be strictly $\frac{\lambda}{2}$. The coupling remains strong enough in the

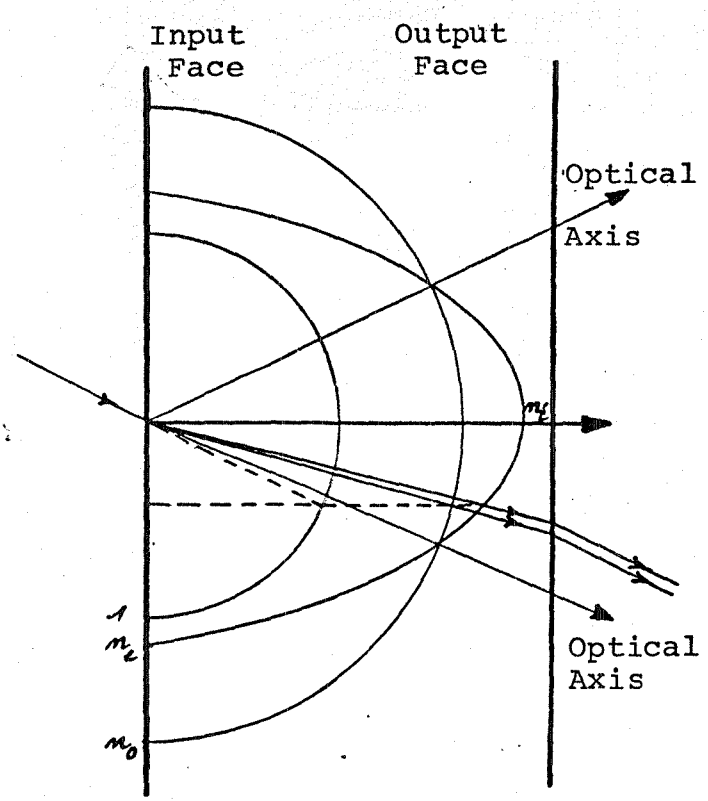

Figure 4 - Refraction In A Biaxial Crystal.

entire fluorescence bandwidth. However, it is feasible to tune the high voltage applied to the Pockels cell as a function of to wavelength to commutate.

The Pockels cell position in the laser cavity is determined on the basis of maximum instantaneous power density considerations. In the first experiments, the cell was placed between the dye tank and the afocal system. After a few hours of operation, the crystal was pitted at the center. /10

Let us evaluate this power density.

The oscillator is pumped with 3 mJ on the average during testing. If its output is 10% rated capacity, it ejects an energy level of 300 μJ for 20 ns, or an average power of 15 kW. Even though the output mirror has a reflection coefficient of 4%, it must be assumed that this power exists in the cavity.

Knowing that the beam diameter is about 0.3 m/m, the mean power density is equal to 17 MW per cm^2.

It is now necessary to account for two form factors, time and space, which express the non-uniformity of the beam, according to these two dimensions. The first is hard to measure, because if it is easy to observe a very large modulation in the light from the oscillator, the bandwidth of our analyzer does not enable us to offer an exact evaluation of the ratio between the peak value and the mean value.

An examination of the shape of the Yag laser pulse shows a virtually 100% sinusoidal modulation. Accordingly, the ratio we are looking for must be close to 2. The power density already reaches 34 MW/cm^2.

The second shape results from the study of the energy distribution in a straight beam section at the crystal level. If it introduces a heat lens effect in the dye tank, this factor may reach a high value which perfectly explains the destruction of the Pockels cell in certain cases.

The Pockels cell being placed between the telescope and the grating, like the Glan prism, it must have certain qualities relative to its optical homgeneity. If these components exhibit prismaticity faults, these may always be compensated by rotating the mirrors. Conversely, if the faults affect the planeness of the wave, and therefore the direction of the light rays, the incidence over the grating will be modified and we will observe a boradening of the spectral line. We must not forget that the theoretical resolution from the grating is actually acheived only when it is illuminated by a plane wave. Rayleigh's criterion is therefore applicable to each of the components found between the afocal and the grating.

I - 2.3. Afocal System

Let us evaluate its residual chromatism. This system offers a Clairant-Mossoti type achromatic and aplanatic doublet and a plane-concave silicon lens. From 300 to 700 nm, the silica index and therefore the focal line of the lens vary as shown in the table below:

λ_{nm}	n	f_{mm}
300	1.4874	2.052
500	1.4628	2.161
700	1.4561	2.193

Suppose we have an afocal system for λ = 500 nm, let us calculate the beam divergence on the dye tank side, when the wavelength has extreme values:

λ_{nm}	300	500	700
divergence	17'	0	10'

Knowing that the widest known fluoresence band is that of rhodamine (38 nm), we may estimate the maximum divergence introduced by the residual chromatism of the telescope as we move away from the center of the band: /12

λ range	Maximum Divergence
300 to 500 nm	1'.6
500 to 700 nm	0'.8

The beam divergence estimated to be 7'.2 on the lens side of the telescope becomes fifty times greater on the tank side, i.e. 6'. The chromatism influence of the divergent lens is therefore fairly negligible.

Let us add that the longitudinal residual chromatism of the lens (the spectrum is bent) is 100 μ from 450 to 500 nm and 200 μ 500, to 600 nm. In the second part of the spectrum the two focal lines vary in the same direction, there is therefore partial compensation. In the first part of the spectrum, the lens effect is also negligible.

I - 2.4. The Dye Tanks

Two types of dye flow tanks were tested in the same oscillator configuration. The first had a parallelepipedal structure and all of its windows were perpendicular to the light beams. The second one was cylindrical and all of its windows were sharply inclined.

The shortcomings of the second solution are:

-the sharp inclination of the windows made it necessary to rotate the tank when the solvent was changed. The angle of incidence i of the light beam over the window inclined by α with respect to the tube's axis is given as a function of the solvent index by:

$$\sin i = n \sin \alpha$$

The following table was established for the solvents actually used: /13

Solvent	Index	$\alpha = 18°70$
Methanol	1.328	25°19
Water	1.333	25°24
Ethanol	1.361	25°87

The maximum rotation reaches 0.68 degrees, or 41 arc minutes, a much higher value than the beam divergence.

-The mechanical structure prevents part of the dye from being pumped by the YAG laser beam and therefore introduces supplementary losses in the cavity.

I - 3. Study of The Oscillator

The study, adjustment and operation use of the methods of evaluating the pulsed laser beams are recorded in the preceding reports.

The essential points are reviewed below (figure 5).

The beam from the YAG laser (or pumping beam) passes through the first prismatic non-treated glass plate, inclined at an angle of 45°. The light being polarized in the plane of incidence, the fraction R of energy sampled varies rapidly with the angle of incidence and for this reason this angle must be accurately known. From the

measurement of the quantity of energy E_R reflected by the first face of this plate, we may calculate:

-the energy issuing from the YAG laser: $E_y = E_R \times \frac{1}{R}$ or 105 E_R in our mounting.

-the energy $E_c = (1 - 2R)\ E_y$ falling over the oscillator sampling plate. In our case $E_c = -.98\ E_y$.

The measurement is performed using a pyroelectrical joulemeter. The sampling plate is identical to the preceding one and is inclinded by an angle of i. Given the reflection coefficent R(i) of this plate, we may deduce the oscillator's pumping energy E_p:

$$E_p = E_R \frac{(1-2R)}{R} R(i)$$

The energy issuing from the oscillator is evaluated using a second joulemeter. When this sensor is removed, the beam is deviated by a total reflection prism on the entrance slit of a monochromator. A photodiode connected to an oscilloscope is placed on the output slit. This system makes it possible to measure the wavelength emitted by the oscillator with an error range of ±1 nm.

The device used to measure the spectral line width inludes an afocal system (divergent + convergent) which develops a plane wave from the beam exiting the oscillator. This wave illuminates a stable interferometric wedge and the fringes obtained are observed on the screen of an oscilloscope via a bar of photodiodes. The wedge thickness is set at 5, 8.7 or 15 m/m, depending on the case. The open spectral interval, i.e. the wavelength displacement separating the two consecutive fringes is given as a function of the wavelength by:

$$\Delta\lambda = \frac{\lambda^2}{2e}$$

I - 3.1. Study of the Different Dyes

Five dyes capable of satisfying the requirements of of the lidar sensing of the atmosphere were taken into consideration. They are:

-Rhodamine 560 + ethanol,
-Rhodamine 590 + water,
-Rhodamine 610 + methanol,
-Kiton red + methanol,
-Rhodamine 640 + methanol.

For some of these (Rhodamine 560, Kiton red), it was first necessary to try to find the optimum concentration. /16

The experiments started in the configuration in figure 6.

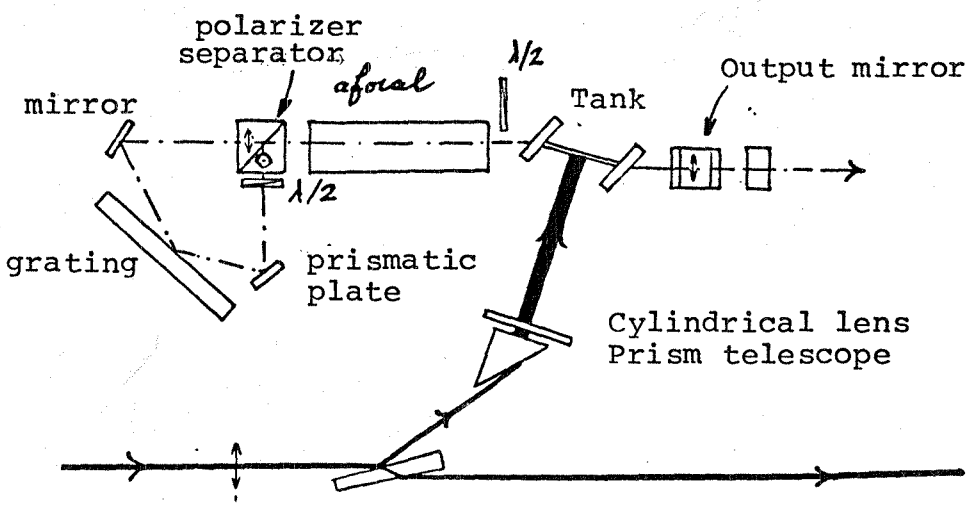

Figure 6 - First Configuration Of The Oscillator.

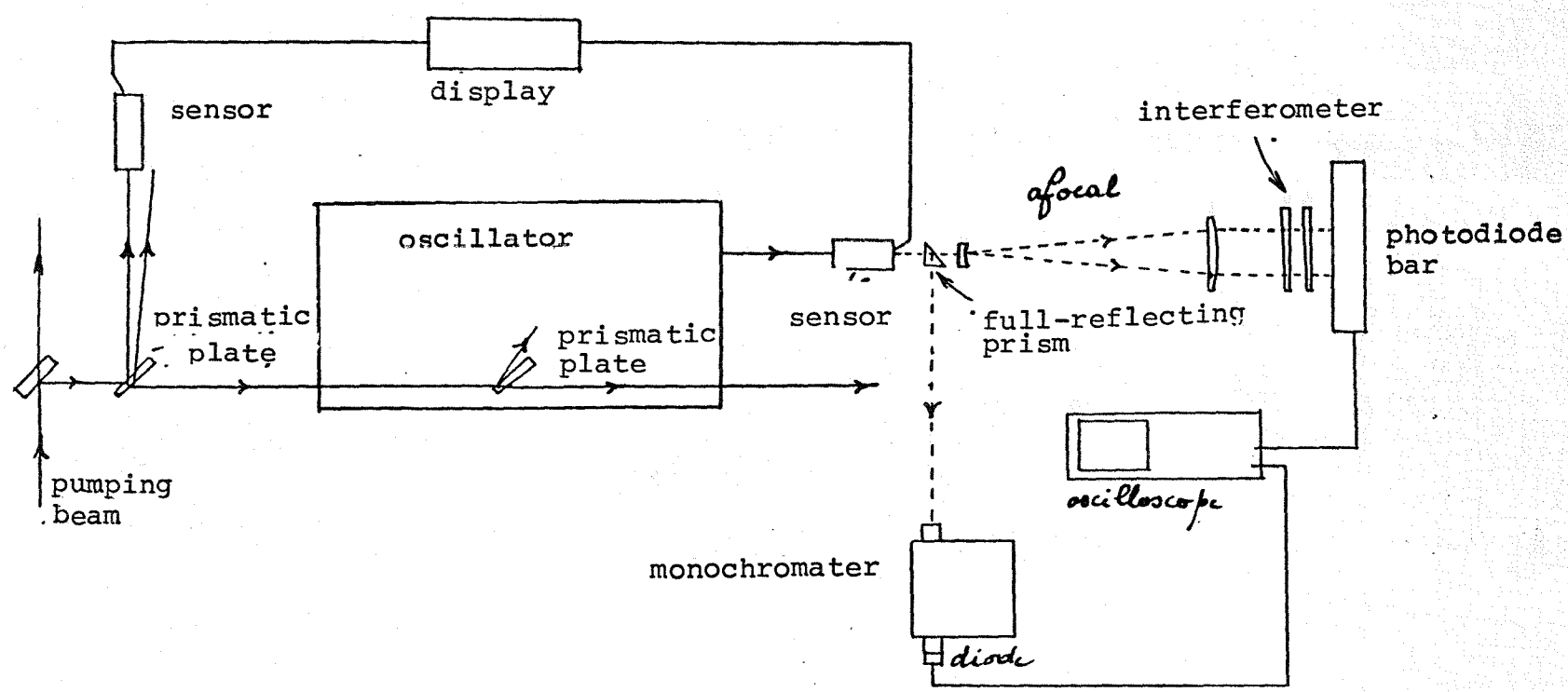

Figure 5 - Oscillator Metrology

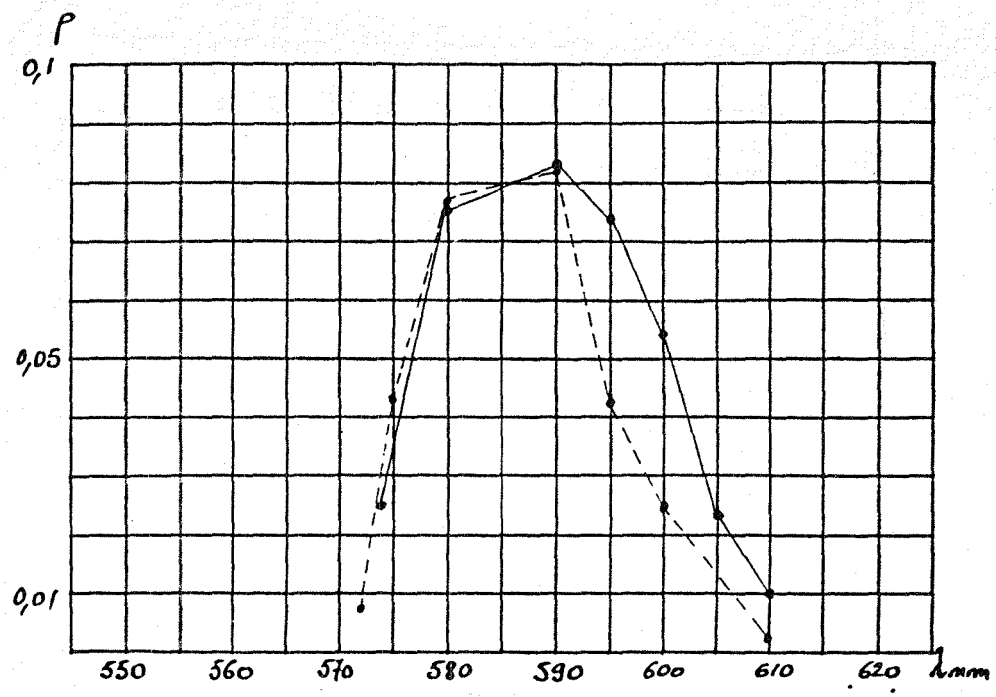

c = 5.3 10^{-4} M/l Ep* = 3.5 mj

——— channel 1 ----- channel 2

Figure 7 - Rhodamine 590 (water & ammonyx L.O. 4%

We prepared a highly concentrated solution (3.58 g/l or 9.75.10^{-3}M/l) which we progressively diluted by watching the conversion efficiency in the oscillator at 568 nm and on channel 1 (figure 9). For the optimum concentration of 1.33 g/l, or 36.10^{-3}M/l, we established the curves in figure 10.

d) Kiton red (P.M. 581) /20

We tried to optimize the concentration in water (+ ammonyx) for an operation at 605 nm. The initial concentration being 0.524 g/l, or 9.10^{-4} M/l. Figure 11 shows that the value we are looking for is 5.6.10^{-4}M/l, but the yield is very low.

*Pumping energy.

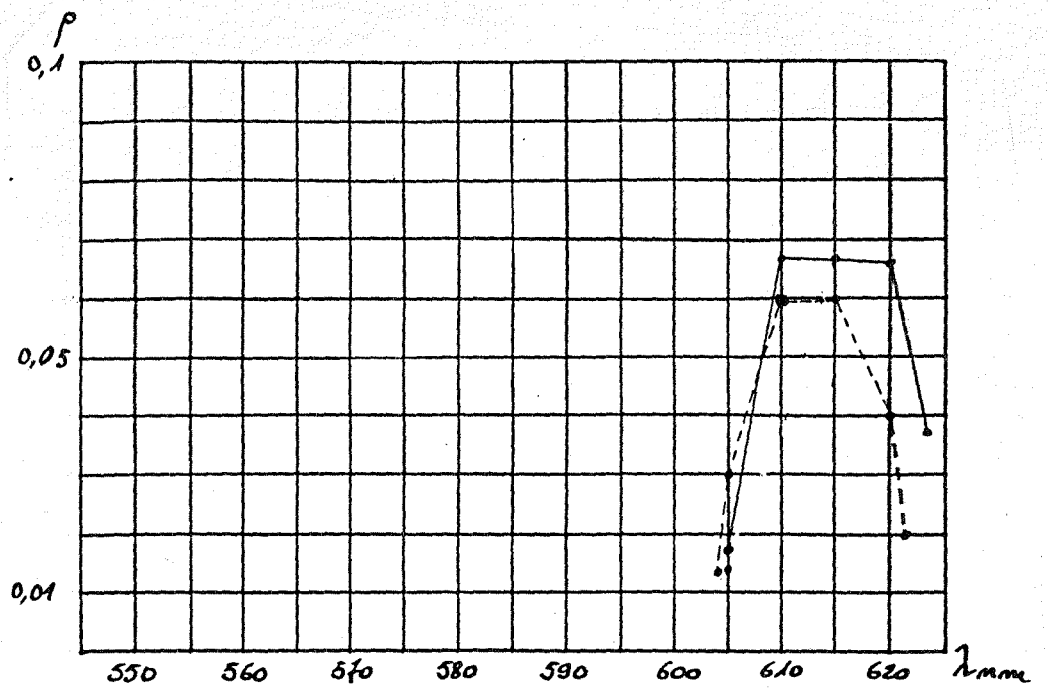

/18

c = 5 10^{-4} M/1 Ep = 3.5 mJ ——— channel 1
----- channel 2

Figure 8 - Rhodamine 640 (methanol)

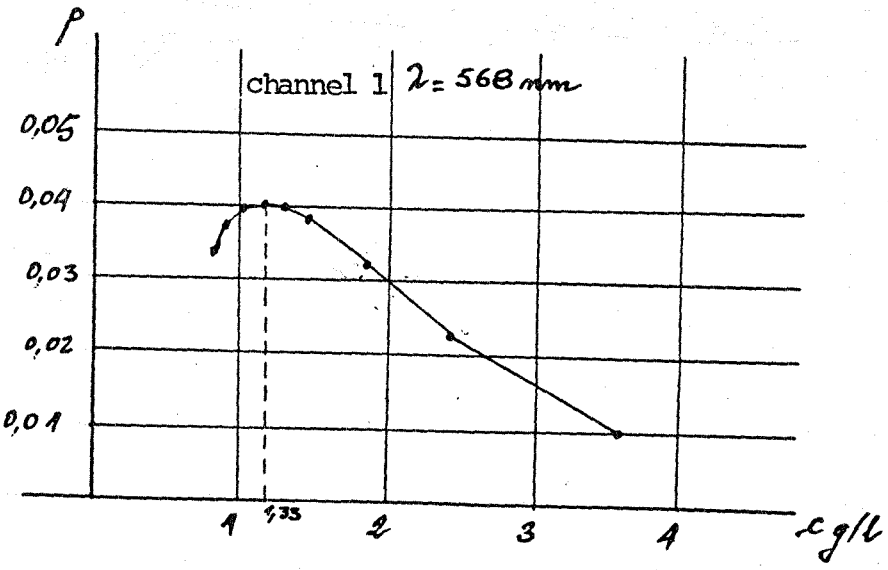

/19

Figure 9 - Rhodamine 560: optimization.

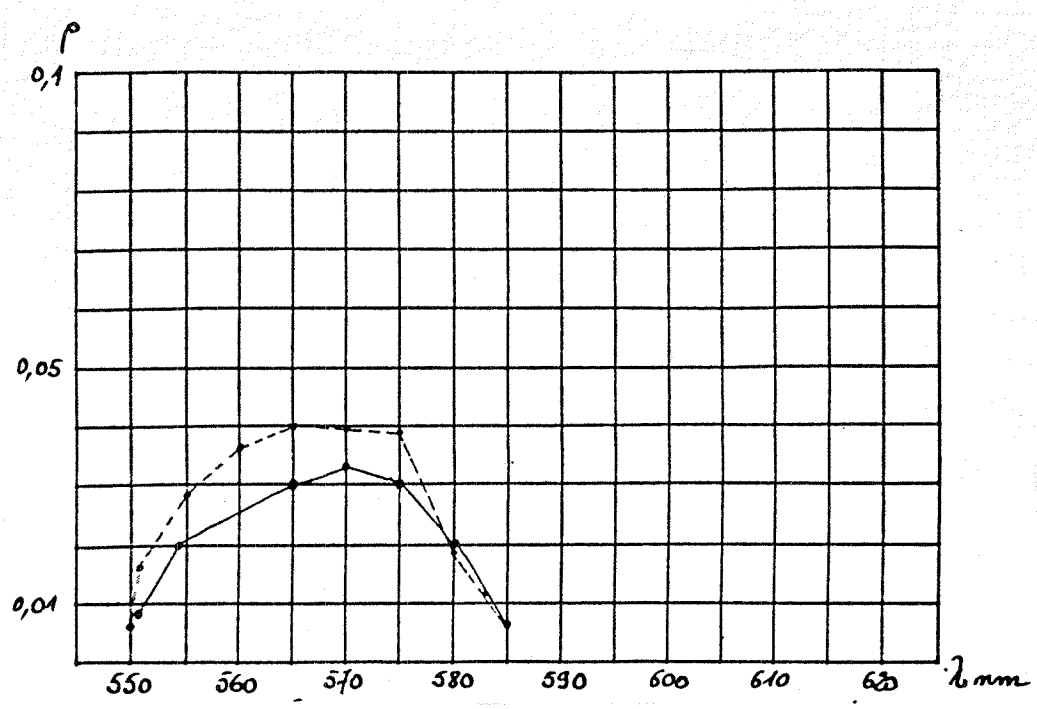

c = 3.6 10^{-3} M/l Ep = 3.5 mJ ——— channel 1 ----- channel 2

Figure 10 - Rhodamine 650 (ethanol)

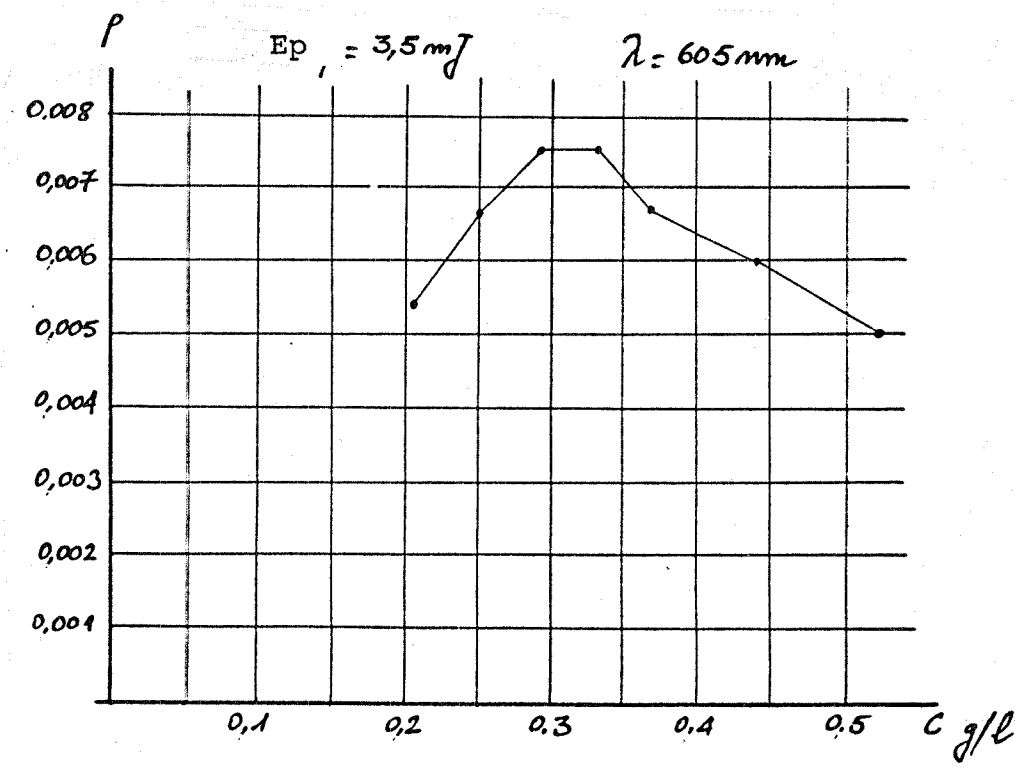

Figure 11 - Kiton red and water: optomization.

Conversely, in methanol, the solution has an almost 10 times better yield. For the same wavelength, we found an optimum concentration of 0.369 g/l, or $6.4.10^{-4}$M/l (figure 12). This dye having a wide fluoresence band, we next tried to find the concentration for which the largest wavelength coincided with the maximum incidence over the grating. Accordingly, we set channel 1 at 620 nm.

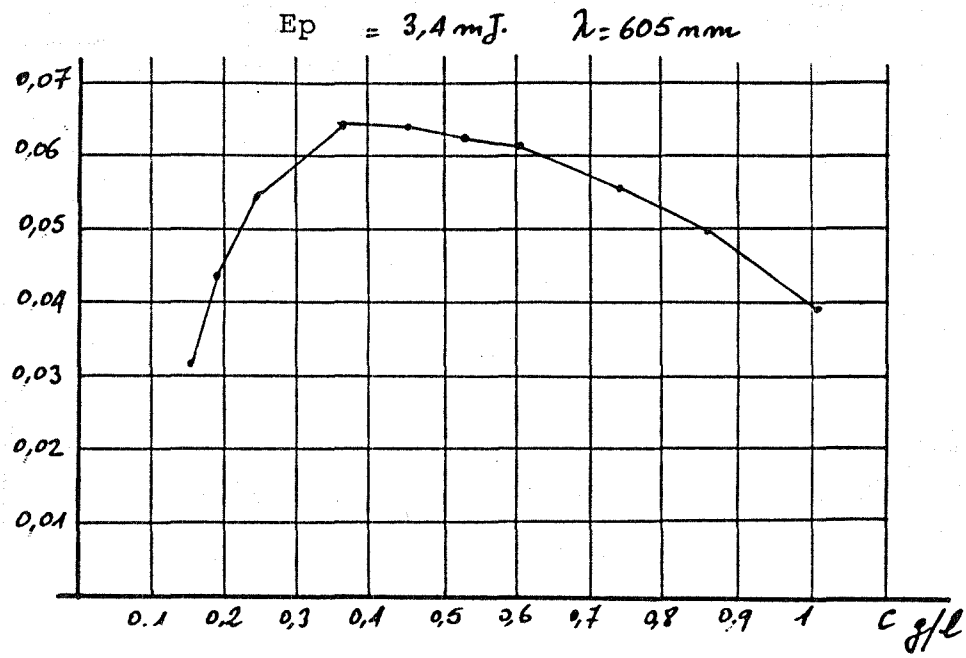

Figure 12 - Kiton red (methanol): optimization.

Starting with the previously found concentration, we progressively diminished it until we had a yield of 2% over channel 1. At the same time, we looked for a low wavelength over channel 2, so that the yield not be less than 25. The results are gathered in the following table.

c	0,369 g/l	0,326 g/l	0,276 g/l	0,240 g/l	0,221 g/l	0,205 g/l	0,185 g/l	0,167 g/l
chan.1 620mm	4,8 %	4,1 %	3,6 %	3,1 %	2,9 %	2,6 %	1,88 %	1,2 %
chan.2			597mm 0,6 %	597mm 0,7 %	597mm 5,5 %	589mm 2,5 %	588mm 2,15 %	588mm 1,8 %
					589mm 1,4 %	588mm 0,84 %		

Ep = 3.5 mJ /21

Figure 13 - Kiton red: tuning band.

The desired concentration is 0.184 g/l or $3.2.10^{-4}$M/l. /22
Finally, we determined the yield curves for this concentration and they are shown in figure 14.

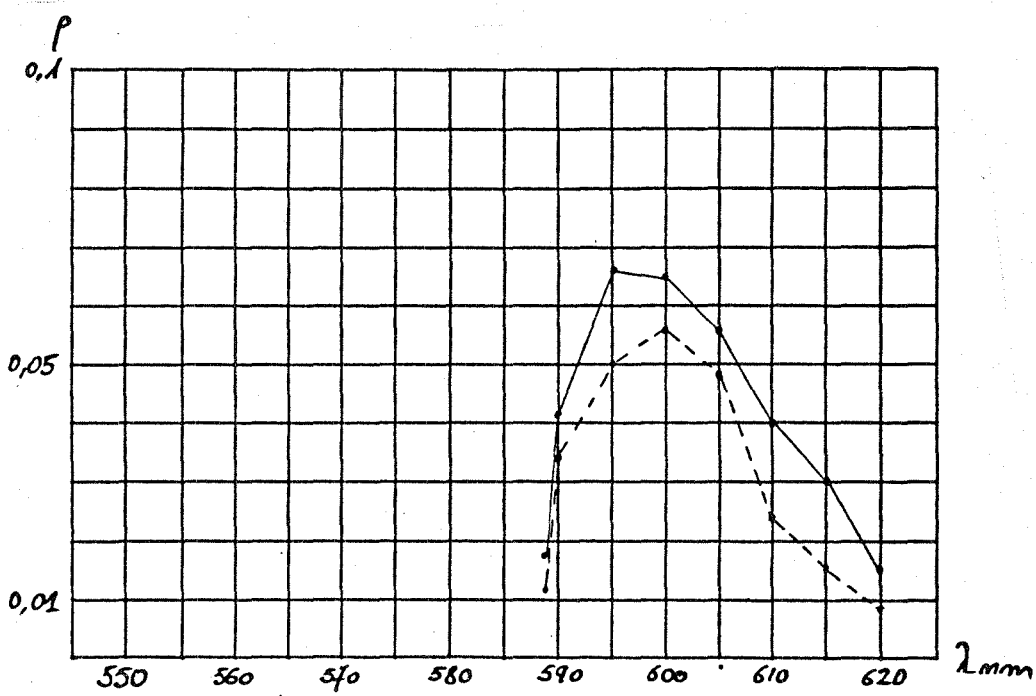

c = $3.2\ 10^{-4}$ M/l Ep = 3.4 mJ —— channel 1
--- channel 2

Figure 14 - Kiton red (methanol)

The polarization separator with dielectric layers is not a "wide band". A supplementary manipulation (figure 15) made it possible to measure the deviation (i) of a polarized beam p relative to the normal as a function of the wavelength, so it may be "extinct" over path s.

λ_{nm}	620	615	610	605	600	595	590	586	585	575
i°	0	0,69	0,99	1,68	2,17	2,95	3,39	4,02	4,47	5,32

/23

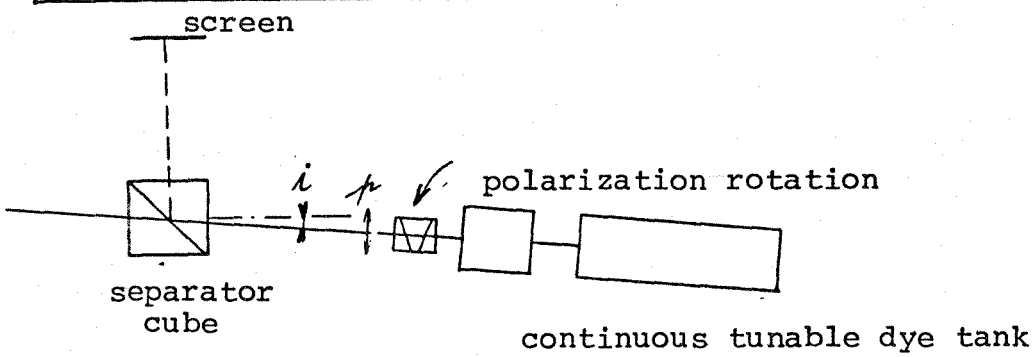

Figure 15 - Study of the polarization separator.

From the conclusions of this experiment, we decided to replace this component with a Glan prism and therefore to give the oscillator the second configuration shown in figure 16.

c) Rhodamine 610 (P.M. 543.02) /24

For this dye, the curves in figure 17 were obtained with a concentration in methanol of 0.18 g/l, or $3.3.10^{-4}$ M/l.

While retaining the same overall oscillator configuration, we replaced the cylindrical structured tank with a parallelepidedical structured tank. This operation forced us to modify the orientatation of the pumping beam.

/23

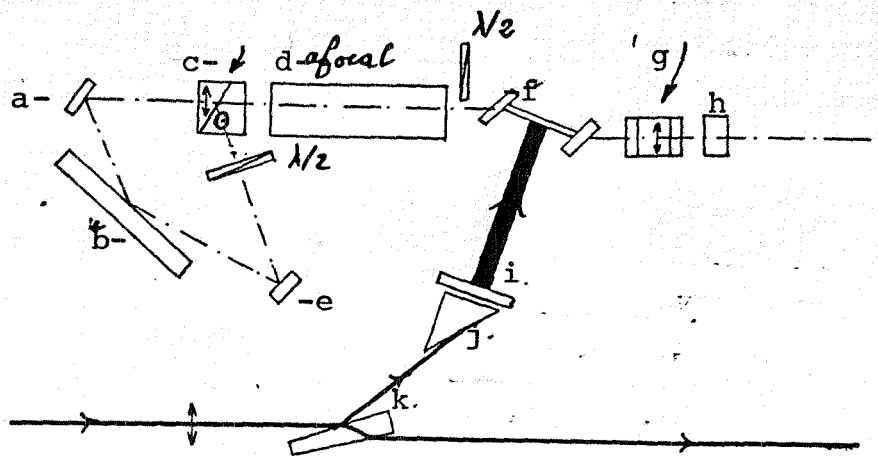

Second Oscillator Configuration

Key: a-Mirror; b-Grating; c-Glan prism; d-Afocal; e-Mirror; f-Tank; g-Polarizer; h-Output mirror; i-Cylindrical Lens; j-Prism Telescope; k-Prismatic plate.

/24

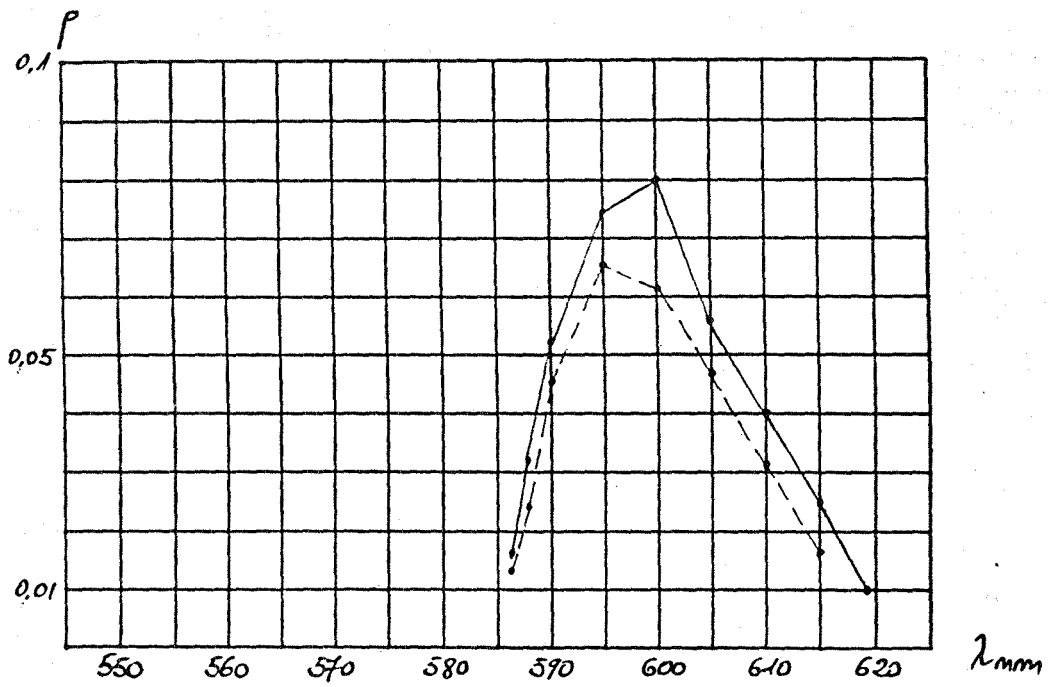

Figure 17 - Rhodamine 610 (methanol)

c = 3.3 10^{-4} M/l; Ep = 2.3 mJ; ——— channel 1
----- channel 2

We also modified the position of the grating, so that with the Glan prism (which deflects the beam by 110°), the lengths of the optical paths in the cavity are the same for both channels (figure 18).

/25

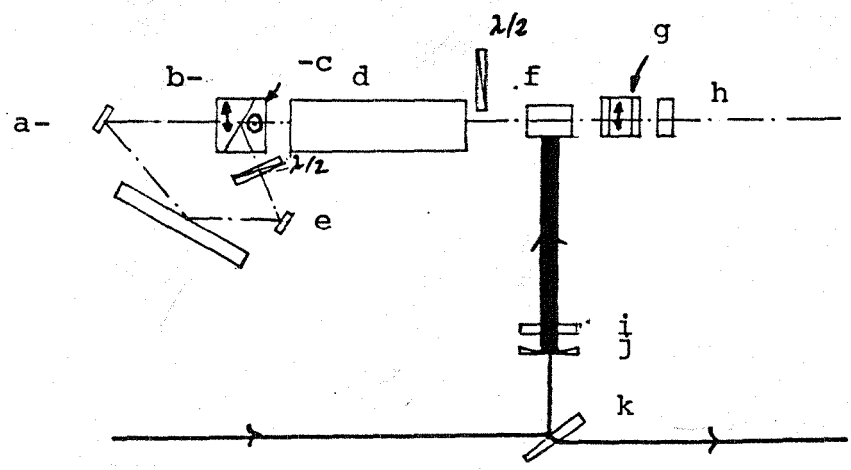

Figure 18 - Installation Of The Parallelepipedal Tank

Key: a-Mirror; b-Grating; c-Glan prism; d-Afocal; e-Mirror; f-Tank; g-Polarizer; h-Output mirror; i-Cylindrical lens; j-Divergent lens; k-Prismatic plate:

I - 3.2. Line Width

The fringe profiles obtained using a photodiode bar placed behind the interferometric analysis wedge are projected on an oscilloscope. Each of the photographic shots shown in the appendix is the superposition of 100 successive profiles (100 shots, or 10 seconds). For lower wavelengths, the grating finesse is lower and we see more longitudinal modes. Conversely, for higher wavelengths, the incidence on the grating becomes grazing and the spectral line is very fine. Actually, from relationship (2) we extract the cosθ value:

$$\cos\theta = \sqrt{1 - \frac{\lambda^2 N^2}{4}}$$

which we replace in (3) with $d\theta = \frac{0.88\lambda}{a}$ which is the diffraction limit (1).

$$d\lambda = \frac{2}{N} \times \frac{0,88\lambda}{a} \sqrt{1 - \frac{\lambda^2 N^2}{4}}$$

This variation of the width of a single pass theoretical spectral line as a function of the wavelength, caused by the grating, is shown by the broken line curve in figure 19. The different measuring points are sometimes below the curve (recirculation or multiple passes over the grating), sometimes above. The error range on the measurement is due to the jitter which occurs on the laser line and which is added to its width during the recording sequence. This jitter is essentially due to the heat effects in the dye tank. /26

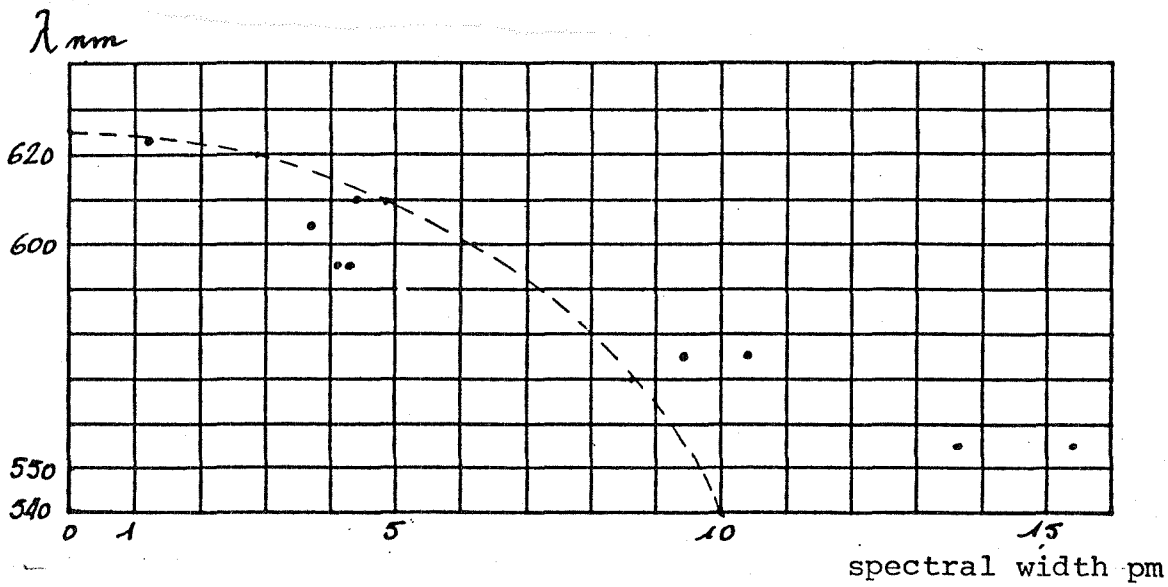

Figure 19 - Line Width & Wavelength

I. - 3.3. Polarization Influence

For the two types of dye tanks studied, we have measured the efficiency variations as a function of the electrical field directions of the pump beam and of the oscillator beam. The figure below represents the positions of the electrical fields. That of the oscillator is defined by the polarizer position, while that of the YAG laser is defined by the position of a half-wave plate.

In the case of the cylindrical tank, the efficiency is reduced to the incident power on the cylindrical lens to eliminate the prism transmission coefficient which varies from 0.73 to 0.43 as a function of the polarization.

For the parallepipedal tank, the sampling plate is at 45°. The prism is replaced by the divergent lens in order to adapt the pump beam to the diameter of the tank's entrance window.

The table below gives the comparative yields over the two channels for the Kiton red at 600 nm. /27

Polarization	Channel	Cylindrical Tank		Parallelepipedal Tank	
		Ep	ρ	Ep	ρ
Horizontal	1	2,6 mJ	3 %	0,6 mJ	1 %
	2		2,5 %		4 %
Vertical	1	7,9 mJ	7 %	5 mJ	7 %
	2		6 %		7 %

The yield is better when the electrical field vectors are colinear in the dye. Owing to this observation, and in order to minimize losses in the cavity, we ordered a polarizer with an entrance face at Brewster's angle, while the other face remains perpendicular to the beam and serves as an output mirror.

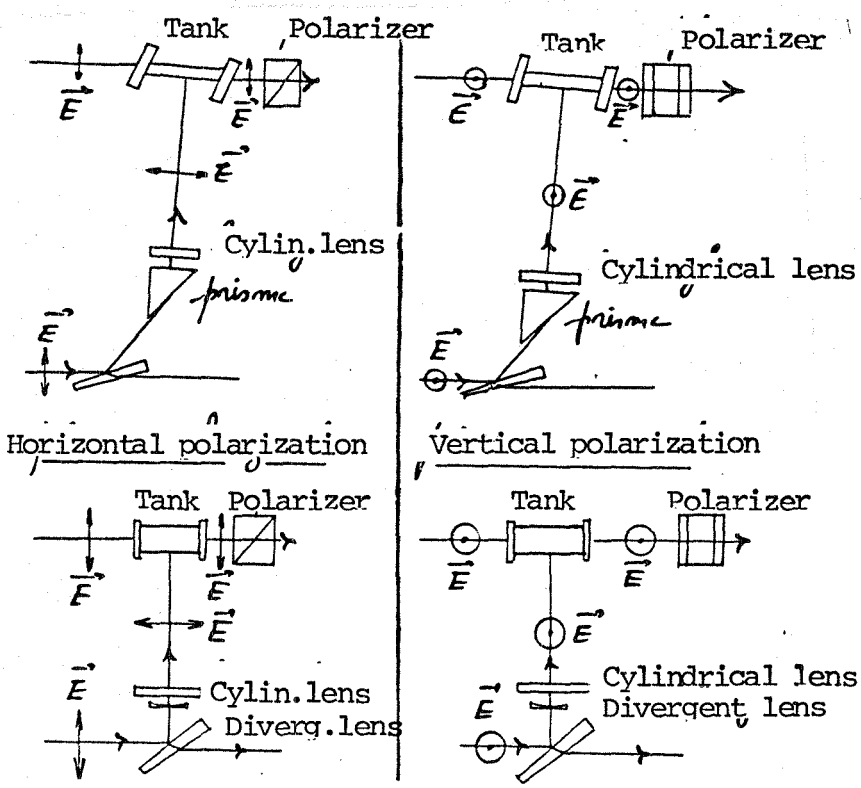

Figure 20 - Polarization Influence

Owing to the dispersion in the calcite, the direction of the beam coming out may change as a function of the wavelength. /28

The table on the next page serves to calculate the maximum shift between 500 and 800 nm.

For a band of 20 nm, the dispersion of the extraordinary

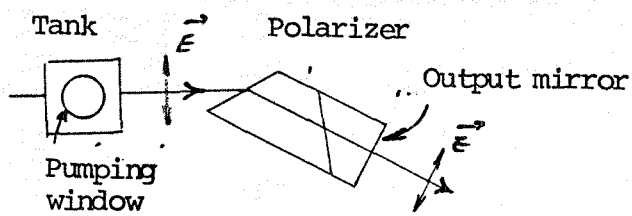

Brewster's Polarizer

λ	n_e	n_0
508	1,48956	1,66527
643	1,48490	1,65504
706	1,48353	1,65207
801	1,48216	1,64869

index for calcite is: $\Delta n_e(38\ nm) \pm 9.6.10^{-4}$. On the polarizer's input face, the angles of incidence and of refraction are given by: $\sin i = n_e \sin r$. By differentiation, we find that the variations of the refraction angle are associated with the index variations by:

$$dr = - tg^2 \frac{dn_e}{n_e}$$

and the angle of emergence i' varies as follows:

$$|di'| = tg\ r\ dn_e$$

At Brewster's incidence tg r equals about 0.6. When the wavelength varies the beam deflection is: $|di'| = 0.6\ dn_e$.

If we assume that the polarizer is adjusted for the center of the fluorescence band of rhodamine 590, the deflection at the ends of the band should be $2.9.10^{-4}$ radian, or about 1', which is a much lower value than that of the divergence of the beam issuing from the oscillator. /29

With the latter component, the oscillator assumes the configuration shown in figure 1. Note that the beam leaving the oscillator deflects downward. There is perhaps a solution by using prisms to make it colinear to

the cavity axis, but we have chosen to couple the oscillator and the amplifiers with two mirrors. This arrangement offers the advantage of increasing the distance between the oscillator and the first amplifier and, next, to decrease the fraction of super-fluorescence which rises through the amplifers to perturb the entire laser operation.

I - 3.4. Tuning The Oscillator

The different manipulations made it possible to develop an oscillator tuning procedure.

After removing the afocal system, the image distance of the cylindrical lens is set to obtain the smallest possible pump volume. A low pump power is used.

After placing a screeen between the dye tank and the afocal system, the orientation of the cylindrical lens and the polarizer is adusted so that the amplification of the fluoresence is level with the window of the dye tank. The pump power is progressively reduced until the optimum seting is achieved.

By removing the screen, the beam should reach the center of the grating along channel 2. Excitation is obtained by tilting the deviating mirror only about the axis perpendicular to the grating lines. To achieve this, it is necessary for the half-wave plate to be correctly oriented. The wavelength is modified by rotation about the other axis.

After replacing the afocal system, the dye tank-cylindrical lens system is set in motion (translational only) in order to center the pumped volume over the axis of the

afocal system, and via a screen placed over channel 2, over channel 2. Another attempt is made to obtain oscillation excitation, then the Pockels cell is correctly put in place. /30

If it is not prismatic, its setting does not put the oscillator out of adjustment. Depending on its orientation, it is switched on or off to open channel 1 and we try to generate oscillations by tilting the corresponding mirror about the axis perpendicular to the grating lines.

II - THE DUAL FREQUENCY LASER

Figure 21 shows the general scheme of the dye laser and the devices used to measure energy, the wavelength emitted, the spectral line width.

In its initial version, the laser was optimized at 590 μm with the rhodamine 590 nm. Dissolution difficulties made us decide to prepare first a concentrated solution in methanol. Then, we added water to obtain the required concentration, while the methanol disappared little by little by evaporation.

II - 1. The Setting: is achieved in two parts: /32

The first one consists of suitably aligning the 3 amplifier tanks and the volumes pumped in each of them. To achieve this, the oscillator is isolated from the amplifiers with a screen and the superfluoresence energy exiting the laser is measured. It must be at a maximum level. Since this fluoresence is also amplified in the amplifier - oscillator direction, we observe an impact on deviating mirror B by removing the screen and preventing the oscillator from pumping.

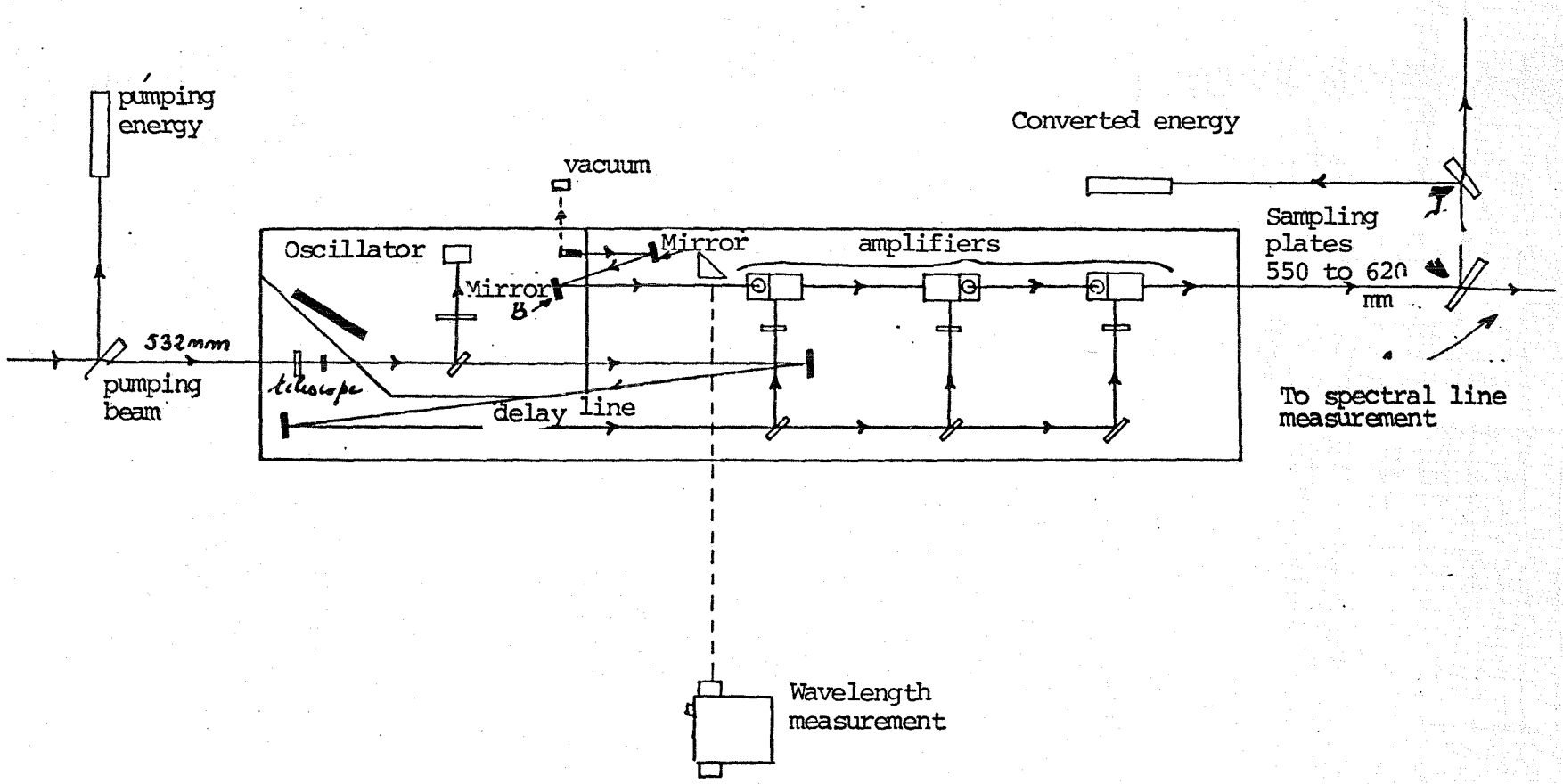

Figure 21 - General View Of The Dye Laser
(Scale About 0.1)

The second part consists of rendering the beam from the oscillator indistinguishable from the fluorescence beam. When this is achieved and if the energy supplied by the oscillator is enough, the fluorescence disappears and is replaced by the laser amplificating. By orientating deviating mirror A, the impact of the oscillator beam is superposed with that of the fluroscence over mirror B and by orientating mirror B, we direct the oscillator beam in such a manner that it passes through the three amplifying tanks.

With concentrations of 4.5 lo^{-4} m/l in the oscillator and 1.5 10^{-4} mol/l in the amplifiers, we have obtained a 48% efficiency on the 2 channels before inserting the Pockels cell. After inserting it, we achieved a yield of more than 30% on the 2 channels between 573 and 601 nm. We noticed that the oscillator should furnish at least 1.5 mj in order to suitably regulate the amplifier chain.

If the oscillator beam is too divergent, a lens can be added in front ofthe first amplifier. A better regulation is thus assured.

II - 2. Changing Dyes: We replaced the rhodamine 590 with Kiton red in the following concentrations:

oscillator: 1.310^{-3} m/l,
amplifiers: $3.2\ 10^{-4}$ m/l.

Under these conditions, we achieved a 35% yield on channel 1 at 604 nm and 32% on channel 2 at 617 nm.

II-3. Problems Associated With The Pumping Laser /33

II-3.1.

The results were obtained with energy from the pulses of the pump laser not exceeding 180 mj in the green for 600 mj in the infrared.

Following an operator intervention, this pump energy regained its nominal value of 250 mj.

After filling the circuits with rhodamine 590 in the following concentrations:

oscillator: $4.5\ 10^{-4}$ m/l,
amplifiers: $1.5\ 10^{-4}$ m/l,

the yield was limited to 30% on both channels at 590 nm for reasons of partial destruction of the lenses and of the pumping shield windows. The spectral analysis of the beam exiting the dye laser shows no trace of fluorescence.

II-3.2.

The Pockels cell of the dual frequency oscillator is triggered by a synchronization signal from the YAG laser (figure 22). However, the light pulse from this laser exhibited an erratic jitter prior to the intervention and this delayed the wavelength modification tests during the pumping pulse. A few incomplete trials were implemented.

A vacuum diode placed above the output polarizer of the oscillator (figure 21) receives the fraction of radiation reflected on the face inclined to Brewster's angle and enables the time factor of the pulse to be controlled.

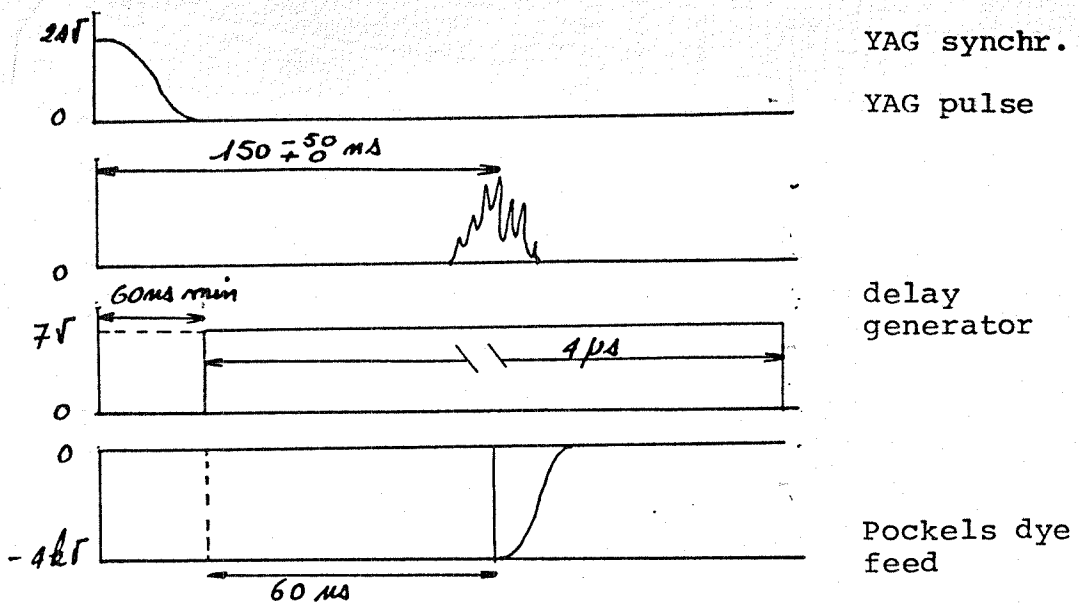

Figure 22 - Electrical Signals

When the Pockels cell is regulated to modify the wavelength in the middle of the pumping pulse, a "Q switch" phenomenon is visible in the oscillator: the pulse assumes a much higher peak value. On the spectral analysis interferometer, the two spectral lines appear with much less contrast: one is tempted to say that they are widened or that the gain has diminished in the oscillator because their number of recirculations (multiple passages) has decreased.

To ascertain this, further testing shall be performed with much finer laser lines, namely, higher wavelengths.

The experiments will be suspended a few months during which the radar will be used to adjust the dual frequency dye emission subsystem.

CONCLUSION

The insertion of a new type of oscillator widening the scope of the dye laser has not appreciably changed the initial performances of the latter. We have eliminated losses in the oscillator as far as possible so that its efficiency (which is still low: 10% at the most) will still allow for an appropriate pumping of the amplifiers. Under these conditions, the superfluorescence which rises in the amplifiers is partially reflected on the oscillator output plate, then "comes back down" through the amplifiers and is "eliminated". Keeping the oscillator a good distance away from the amplifiers is undoubtedly a precaution to take in the preparation of the next model.

The complete chain in the dual frequency version will be tesed with other dyes in the vicinity of 700 nm, then in a second phase, we will replace the pumping at 530 nm by a pumping at 308 nm.

PREVIOUS REPORTS

/35

1. Aubry Y., "Dye Laser Chain - Method of Evaluation," 8/6035 DERO.

2. Aubry Y., "Dye Laser Chain - Method of Evaluation," (continuation) 4/6047 DERO.

3. Aubry Y., "Metrology Of Pulsed Laser Beams," 5/5056 DERO.

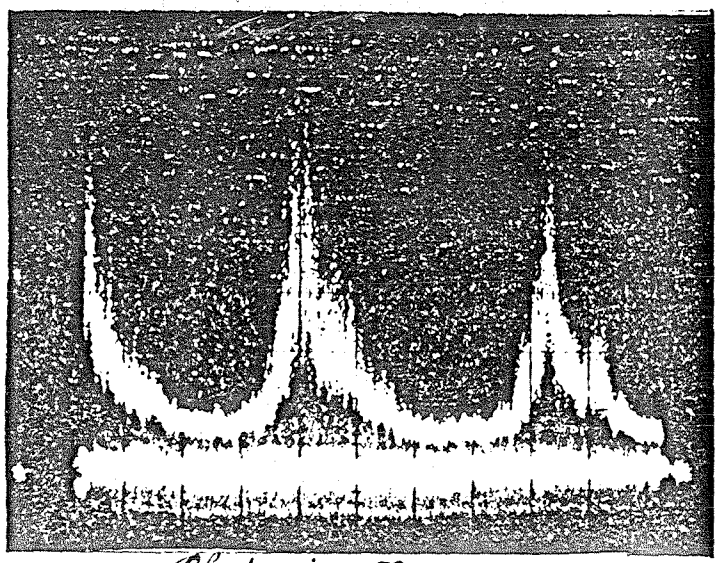

Rhodamine 590 + water
λ = 595 nm channel 1 - free spectr. interval 20.3 pm

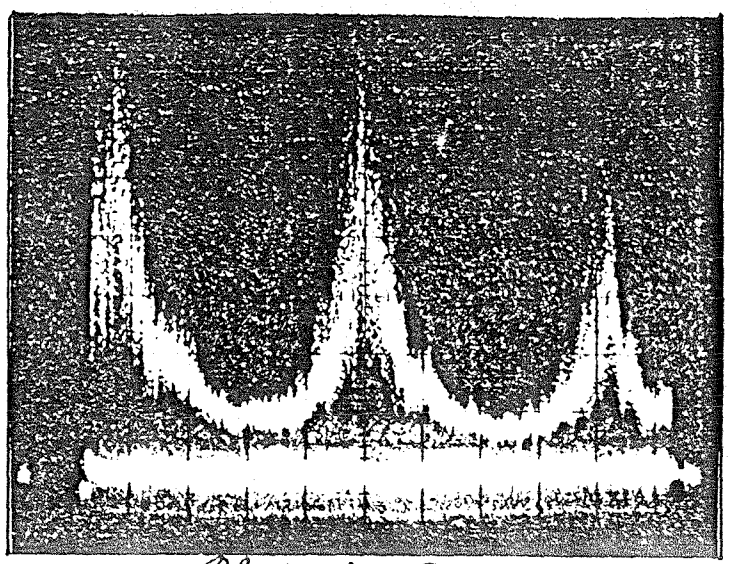

Rhodamine 590 + water
λ = 595 nm channel 2 - free spectral interval 20.3 pm

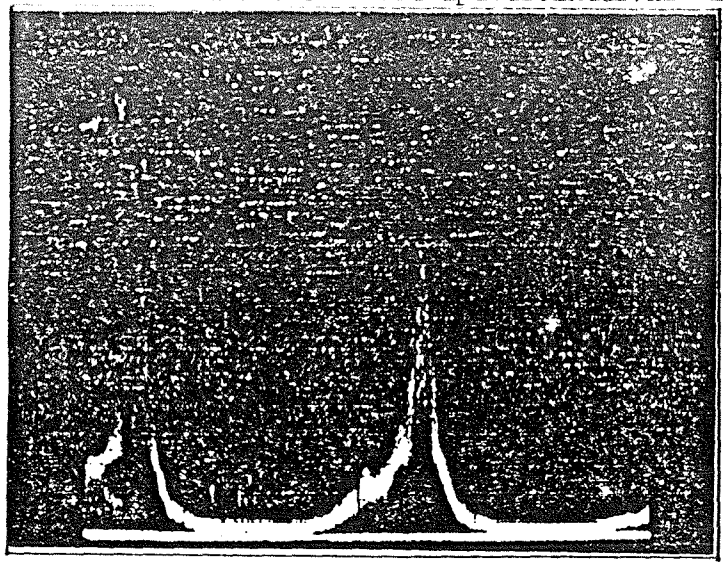

Rhodamine 590 + water
λ = 595 nm channel 1 - free spectr. interval 31.3 pm

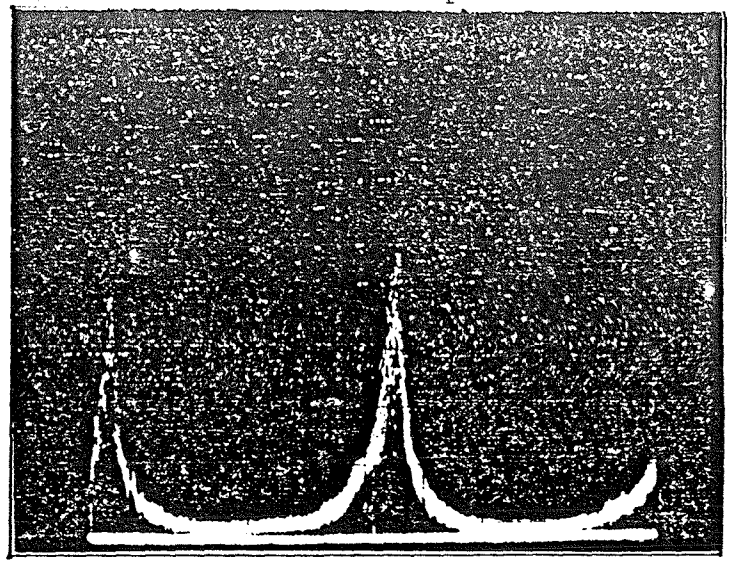

Rhodamine 590 + water
λ = 595 nm channel 2 - free spectral interval 39.3 pm

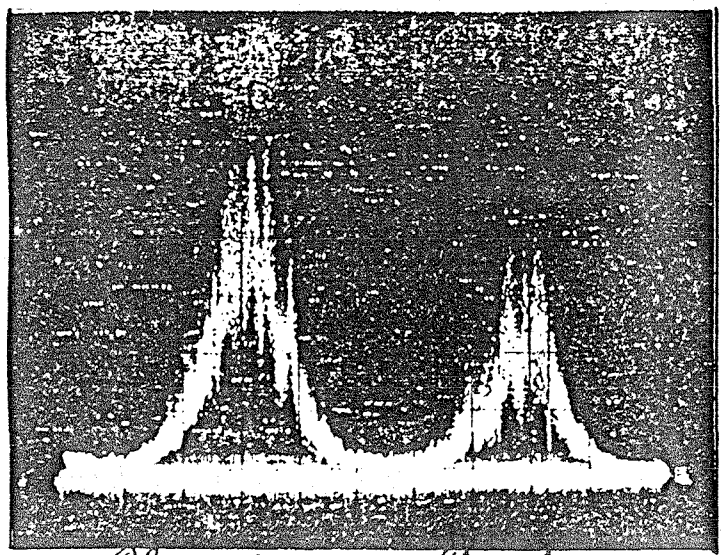

Rhodamine 560 + Ethanol

λ =575 nm channel 1 - free spec. inter. 33pm

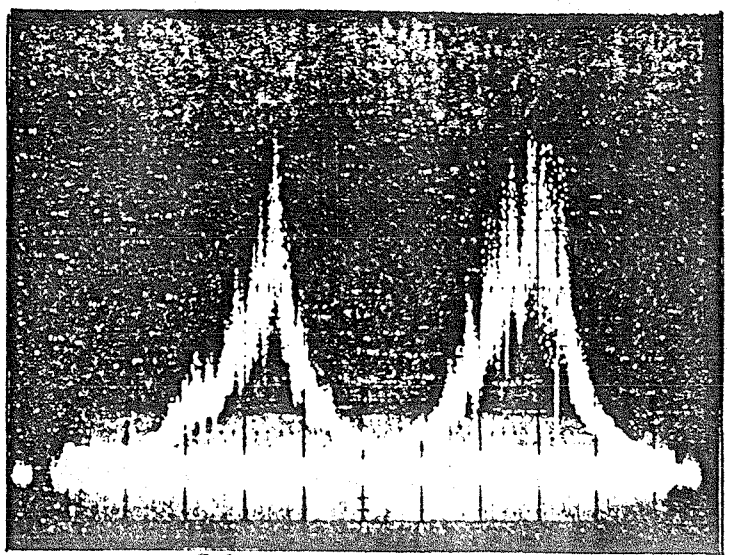

Rhodamine 560 + Ethanol

λ =575 nm channel 2 - free spectral interval 33pm

Rhodamine 560 + Ethanol

λ =555 nm channel 1 - free spectr. inter. 39.8pm

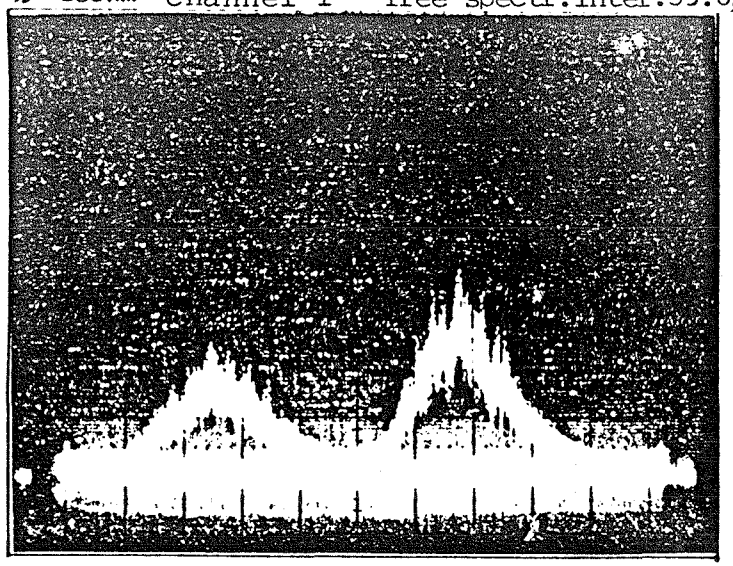

Rhodamine 560 + Ethanol

λ =555 nm channel 2 - free spectral interval 39.8 pm

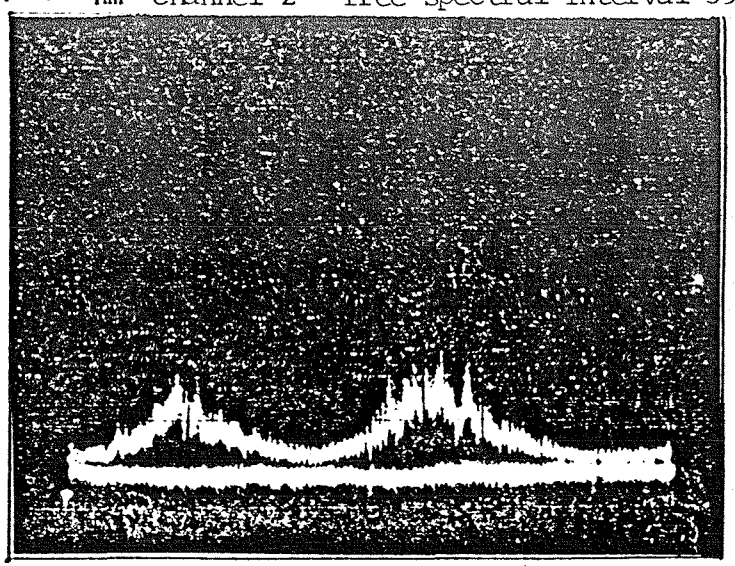

Rhodamine 640 + methanol

λ = 610 nm channel 1 - free spectral inter. 21,4 pm

Rhodamine 640 + methanol

λ = 604 nm channel 2 - free spectral interval - 24 pm

Rhodamine 640 + méthanol

λ = 623 nm channel 2 - free spectral interval 12.9 pm

End of Document